Pinning of graphene to Ir(111) by flat Ir dots

Peter J. Feibelman
Sandia National Laboratories
Albuquerque, NM 87185-1415

Compact, flat, Ir islands form, and are stable to 400K, when <0.1 monolayer of Ir is evaporated onto a graphene flake pre-adsorbed on Ir(111). Local Density Approximation calculations account for the Ir islands' two-dimensionality and their preferred sites on the substrate. They show that local sp^3 bonding at once chemisorbs the dots above the graphene, and pins the graphene layer firmly to the underlying metal.

PACS codes: 68.35.Ct, 71.15.Mb

I) Introduction - Periodic arrangements of adsorbed transition metal clusters offer exciting prospects for applications ranging from catalysis, to information storage and quantum computing. Cluster periodicity may result from self-assembly, i.e., from cluster-cluster interactions,[1] but achieving a thermally stable nano-dot array is more likely[2] when a substrate exposes adatoms to a periodic arrangement of energetic nucleation sites. Just such sites are implicated in

Pd cluster ordering on oxidized Ni_3Al,[3,4] also in Co dot ordering on Au(788)[5] and in a Ni dot pattern on Au(111).[6]

The subject of this article is a subtle example of heterogeneous nucleation, the Ir nano-dots grown by N'Diaye, et al. on large graphene flakes on an Ir(111) single crystal surface.[7,8,9] This well-ordered hexagonal dot arrangement is stable to 400 – 500K (to higher temperatures for larger dots), and moreover, even at the lowest Ir adatom coverages, the Ir dots occupy array sites, whether or not neighboring sites are occupied. Both these behaviors imply that cluster-cluster interaction does not dominate array formation, and thus, they beg the question of what makes a graphene layer on an Ir(111) surface sufficiently heterogeneous to support the observed, periodic Ir nanodot arrangement.

At the outset, this seems quite a mystery. An isolated graphene layer is essentially flat, and, as one knows from graphite's low friction, typically interacts weakly with its ambient. The close-packed surface of Ir metal is weakly corrugated. What can make graphene on Ir(111) interact strongly with adatoms, and what can make the graphene layer heterogeneous?

An initially obscure clue is that because of the mismatch of C-C and Ir-Ir inter-atomic distances, a graphene layer adsorbed on Ir(111) undulates gently, giving rise to a moiré image in scanning tunneling microscopy (STM). In itself, this observation offers scant help; there is no obvious reason that Ir bonding to an

undulating graphene array should be much better than to a flat one. Notwithstanding, STM also reveals that the Ir nanodot arrays grow in perfect registry with the moiré.[7] This *is* a telling observation.

The reason a moiré is seen is that the graphene-Ir(111) interaction, though weak, depends on the registry of C atoms relative to the underlying Ir lattice, and that varies across the moiré unit cell. The Ir nano-dots are found where the registry is such that half the C atoms lie almost directly above Ir surface-layer atoms. Local Density Approximation[10] (LDA) calculations reported herein show that this permits a local re-hybridization of the C-C bonds from sp^2 to sp^3, with a corresponding buckling of the graphene layer, such that every other C atom either binds to an Ir surface atom below it or an Ir adatom directly above. Thus, a graphene flake on Ir(111) is heterogeneous in its ability to buckle and form strong, local sp^3 bonds, and the binding of an Ir dot to the graphene simultaneously pins the graphene layer to the substrate.

The remarkable pinning effect can be seen in Fig. 1, illustrating LDA results detailed later on. Before Ir deposition, the sp^2 bonded graphene layer was weakly attached to the underlying metal, at a 3.42 Å average height above the outer Ir layer much above the ~2.13 Å sum of Ir and C atomic radii that would signal chemisorption. Fig. 1 shows that island formation has depressed the graphene layer locally, into contact with the substrate. The reason is that Ir(5d)-C($2p_z$) hybrids

have replaced C-C π-bonds, with alternate C atoms binding an Ir adatom ~2.05 Å directly above, or chemisorbing to an Ir surface atom ~2.15 Å below. Thus, whereas the uncovered graphene layer "floated" above the Ir(111) surface, the island-covered moiré is firmly bound to it, in an arrangement corresponding to local sp^3 – bond formation.

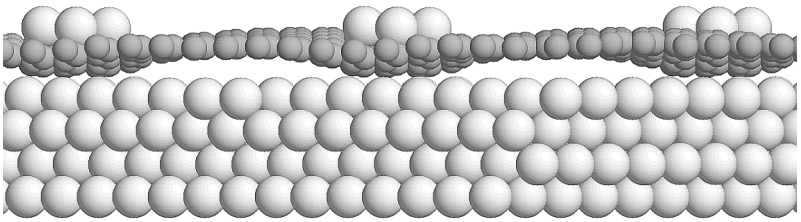

Fig. 1. With ball-model sizes proportional to atomic radii, and balls positioned according to LDA optimization, a side view of a graphene layer pinned to a four-layer Ir(111) slab by a periodic array of four-Ir-atom flat islands. Balls representing Ir atoms are white. Under Ir islands the (grey) C-atoms are in chemical contact with the Ir slab's top atomic layer, but nowhere else.

Although the novel pinning mechanism for Ir islands on the graphene/Ir(111) moiré, and the location of the favored binding sites are the main concerns of this article, how cluster morphology depends on cluster size is also of interest. Ref. 7 made little of the structural energetics of cluster adsorption, even though Density Functional Theory[11] (DFT) calculations based on the Perdew-Wang '91 version of the Generalized Gradient Approximation[12] (PW91-GGA) had been performed, and the graphene buckling signifying a sp^2 to sp^3 bonding

transition was noted. The reason was that flat, few-atom Ir islands were found to be energetically unfavorable compared to pyramidal Ir clusters, at variance with experimental observation. This "accident," attributable to an overestimate of the ratio of Ir-Ir to Ir-C bond strengths in the "PW91-GGA universe," does not occur when one calculates structural energies in the LDA version of DFT. Accordingly, the LDA appears better suited for analyzing Ir island structure on graphene/Ir(111) than the PW91-GGA, and was used in the present work.[13]

Differences in the structural predictions of the GGA and LDA are uncommon, but not unknown – an unfortunate feature of today's DFT state-of-the-art.[14] Having to change functional from one problem to the next undermines the notion that one is working from first principles. Still, such tuning is warranted if the "right" choice of functional not only accounts for key experimental observations (here, the 2-dimensionality of small Ir clusters), but also provides insight into otherwise unexplained atomic-level mysteries (here, the nature of the strong adatom attachment to the moiré and the source of the observed site heterogeneity).

With this rationale, after the review of DFT methods used, in Sec. II, I discuss the calculated energetics of dot morphology (2-d vs. 3-d) in Sec. III. The key structural inferences, and an understanding of island site preference, emerge in Sec. IV from the LDA geometries of 2-dimensional moiré-bound Ir dots. In

particular, calculated bond angles and distances show that $sp^2 \rightarrow sp^3$ rehybridization of C electrons underlies the adsorption of islands comprising more than two Ir atoms, and also causes the graphene layer to chemisorb to the Ir(111) substrate. Ad-cluster site-preference is the subject of Sec. V. Results presented there suggest subtleties in the cluster energy versus location in the moiré cell, and thus, the importance of developing an efficient exploration tool. Sec. VI concerns the binding of small clusters on the graphene layer. Bonding of ad-dimers and monomers differs from that of trimers and larger Ir islands because the former gain little or nothing from Ir-Ir bonding. Sec. VII concludes with further discussion of future projects and directions.

II) DFT calculations – As in Ref. 7, I first optimized the geometry of a 4-layer Ir(111) slab with a graphene adlayer on its upper surface and no Ir adatoms. Experimentally, the graphene overlayer is not strictly commensurate with Ir(111), but a 10×10 graphene adlayer on a 9×9 Ir(111) slab is a good model for the observed moiré cell, which accommodates 87±3 Ir atoms.[7]

Clusters of up to 6 Ir adatoms on the graphene moiré are essentially all planar, according to Ref. 7, whereas, because the Ir-Ir bond is sufficiently strong compared to Ir-C binding, one- and two-layer clusters become equally frequent once the cluster size is as large as 25 Ir's.[15] For the sake of interpreting the Ir-C interactions that bind Ir islands to the graphene layer, I therefore studied small, Ir

adatom clusters in various regions of the moiré. Energy optimization was performed using the VASP, DFT code[16,17] with electron-core interactions treated in the projector augmented wave approximation (PAW).[18,19] I obtained results using the PW91-GGA[10] and also using the Ceperley-Alder version of the LDA (CA-LDA).[20] As noted in Sec. I, only the LDA reliably predicted a preference for small islands to be 2-dimensional.

Using a VASP plane-wave basis cutoff of 400 eV, I fixed Ir-Ir spacings in the bottom Ir layer at the theoretical, bulk value, 2.749(2.701) Å in the GGA(LDA) calculations. (The experimental, room-temperature value is 2.715 Å.) Positions of the remaining atoms were relaxed until none experienced a force of magnitude $>$ 45 meV/Å. I accelerated electronic relaxation with Methfessel-Paxton, Fermi-level smearing (width = 0.2 eV),[21] and corrected for the unphysical contact potential difference associated with having a graphene adlayer on only one side of the Ir slab.[22]

Despite the large, Ir(111)-9×9, moiré unit cell, the ~20 eV width of the occupied 2s-2p bands of graphene makes it desirable to test the convergence of surface brillouin zone (SBZ) sampling. Accordingly, I compared total energies of cells supporting Ir ad-tetramers at various sites, using equally-spaced, 1×1, 2×2, and 3×3 SBZ samples (each including the point, $\overline{\Gamma}$). The results indicated that the 1×1 sample reliably predicts the energy ordering of the different sites. Still,

comparing the 2×2 or 3×3 results to energies computed using the $\overline{\Gamma}$ –only sample showed that the latter underestimates site-to-site differences by as much as 50 meV per Ir adatom. Comparing the 2×2 results to the 3×3 sample's, site-energy differences were < 5 meV/adatom, i.e., an order of magnitude smaller.

Reference to the experimental lattice parameters of Ir and graphite (see Table I) shows that less than 1% strain is incurred in stretching a 10×10 graphene overlayer to match (unrotated) a Ir(111)–9×9 supercell. To gain confidence that the lattice match is equally good in DFT, I optimized the lattice parameter of a single graphene layer, using the CA-LDA and then the PW91-GGA exchange-correlation potential. These optimizations were done using a primitive, 2 C-atom cell, and a 12×12 sample of the corresponding 2-d Brillouin zone. The results confirmed that systematic DFT error in lattice parameters is not a major issue for either DFT implementation. With the GGA-PW91 exchange-correlation potential, a graphene mesh need expand by <0.4% to make the 10×10 graphene cell commensurate with a 9×9 Ir(111) supercell. Closer to experiment, the graphene layer must contract by about 0.6% in the LDA-CA version of DFT.

	$R_{nn;\,Ir(111)}$	$a_{graphene}$	$10a_{graphene}/9R_{nn;\,Ir(111)}$
LDA – CA	2.701 Å	2.446 Å	1.006

GGA – PW91	2.749 Å	2.465 Å	0.996
Experiment	2.715Å	2.462Å	1.008

Table I – Lattice repeat distances for Ir(111) and graphene. The experimental value quoted for "graphene" is actually from an X-ray powder diffraction study of graphite.[23] Weak binding of graphite's graphene layers implies that this is a good approximation.

III) Flat vs. 3-d islands – To capture the full range of morphological results reported in Ref. 7, a theoretical approach must predict that small islands will be flat. Thus, I began the effort to interpret the binding of the Ir clusters by studying 4-atom islands adsorbed in 2-d (rhombus) and 3-d (trigonal pyramid) configurations, as illustrated in Fig. 2. Experimentally,[7] Ir ad-tetramers are stable on the moiré to 400K, and the most abundant cluster size when 0.03 ML Ir has been deposited.

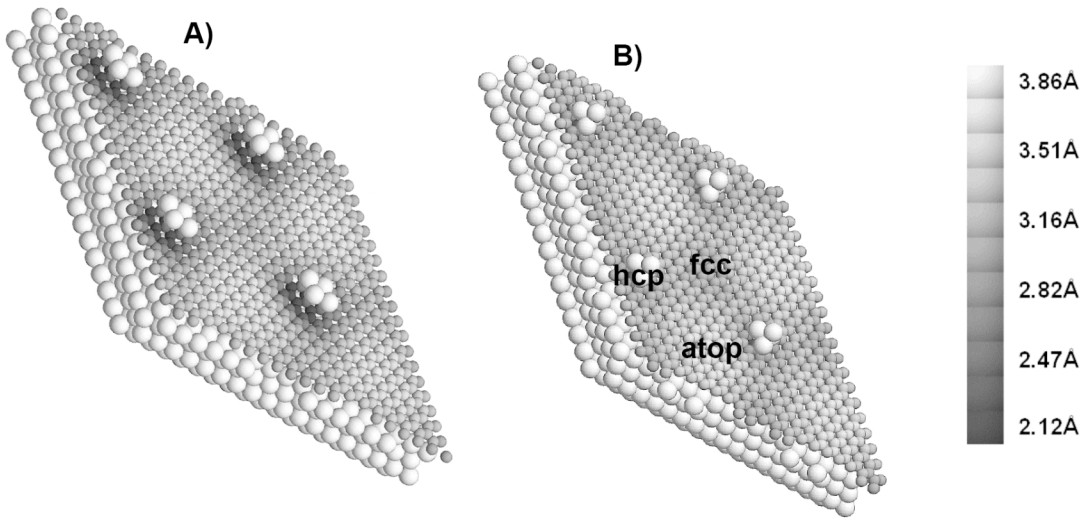

Fig. 2. Four unit cells of the model graphene moiré on Ir(111) decorated by LDA-optimized, A) flat, 4 Ir-atom islands and B) trigonal pyramid islands. Ir atoms are white. C atom heights relative to the average height of the top Ir layer correspond to the grey scale bar. Rings of depressed C atoms surrounding the flat islands of panel A manifest a stronger, induced C interaction with underlying metal than under the pyramidal islands of panel B.

$\overline{\Gamma}$ -only, calculations were repeated for islands centered in the three regions of the moiré where an extremal binding energy might be expected: 1) "*hcp* regions," where rings of C-atoms, alternately in *atop* and *fcc* sites relative to underlying Ir(111) surface, surround 3-fold, *hcp* hollows, 2) "*fcc* regions," where C-atom rings surround an *fcc* site instead, and 3) "*atop* regions," where C's in 3-fold hollow sites, half *hcp* and half *fcc*, surround an Ir surface atom. (See the top view in Fig. 3, left panel, for visual clarification of these definitions.)

Table II summarizes the energies computed in this test. It shows that in both

the *hcp* and *fcc* regions of the moiré, and by significantly more than ½ eV, DFT calculations based on the Ceperley-Alder LDA exchange-correlation potential (CA – LDA) favor flat 4-atom Ir islands over trigonal pyramid clusters. In the *atop* region, the LDA does show a preference for pyramids; but, consistent with the experimental absence of any islands there,[7] it also implies that they are weakly adsorbed – with, in a representative example, a binding energy smaller by better than 2 eV compared to a flat tetramer at its best binding site in the *hcp* region. Thus, Table II implies that the CA – LDA is consistent with N'Diaye, et al.'s observation of flat, small islands, and offers an opportunity to interpret their bonding.

region	$E_B^{LDA}(2d) - E_B^{LDA}(3d)$	$E_B^{GGA}(2d) - E_B^{GGA}(3d)$
"*hcp*"	0.77 eV	–0.87 eV
"*fcc*"	0.61 eV	–0.92 eV
"*atop*"	–0.86 eV	–0.12 eV

Table II – Difference in binding energy between 2- and 3-dimensional, 4-atom islands, i.e., rhombus and trigonal-pyramid islands, centered in the *hcp*, *fcc* and *atop* regions of the graphene moiré on Ir(111) (cf., Fig. 3), calculated using a 1×1 SBZ sample, and either the Ceperley-Alder LDA or the PW91 GGA.

In contrast, the GGA column of the table suggests that in no region of the moiré are flat islands favored over 3-dimensional. Thus, although flat, 4-atom islands may correspond to relative minima in the PW91-GGA potential energy surface, pursuing an understanding of how the observed flat islands bind to the graphene sheet is a less compelling way to proceed.

IV) How Ir islands bind to the graphene layer – The present work has been aimed at two basic questions: How can Ir adatoms bind strongly to what appears, at first blush, to be a relatively inert, physisorbed graphene sheet? And why are adatom islands observed only in the *hcp* regions of the moiré? [7]

Figs. 3 answer to the first question. They show that the graphene layer buckles under a typical LDA-optimized Ir island, in the favored, *hcp* region. This structural distortion signals a local sp^2 to sp^3 rehybridization, from graphene to diamond-like bonding. Amounting to the breaking of graphene π bonds, such rehybridization allows the formation of strong σ bonds between C atoms in *fcc* hollows and the adatoms above them, *and also* between C atoms in atop sites and the metal atoms directly below. Note that island attachment to the moiré is especially strong, because (Fig. 3, right panel) more C-Ir chemical bonds form, locally, than there are Ir adatoms.

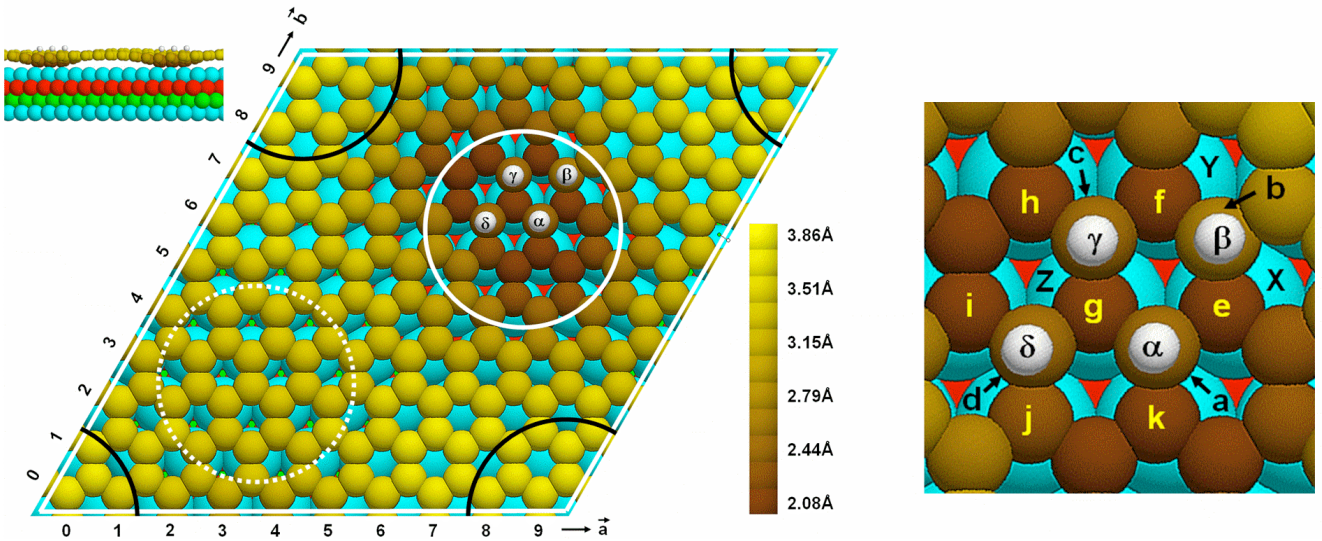

Fig. 3. (Color) Left panel: Computed using the LDA and the 3×3 SBZ sample, the graphene/Ir(111) unit cell with a 4-atom flat, Ir island on it in its lowest energy configuration. First, 2nd, and 3rd substrate layer Ir atoms are colored cyan, red and green (cf., the inset side view). This coloring shows that the solid and dotted white circles encompass the *hcp* and *fcc* regions of the moiré. *Atop* regions, delimited by black arcs, are in the cell corners. Balls representing Ir adatoms are white, and labeled **α**, **β**, **γ**, and **δ**, with radii reduced to reveal ad-Ir registry atop C-atoms in *fcc* 3-fold hollows. Local, island-induced depression of the graphene layer is shown by C-atom coloring; the color bar numerical scale denotes heights measured from the average for the first Ir atom layer. Right panel: A blowup of the immediate island binding region, with atoms labeled to facilitate discussion of bond lengths and angles. Among the C atoms, **e**, **f, g, h, i, j and k** lie low and bind to substrate Ir atoms, among them, **X**, **Y**, and **Z**, while **a**, **b**, **c**, and **d**, lie high and bind to Ir adatoms **α**, **β**, **γ**, and **δ**. Distances and angles drawn from this figure indicate a locally sp^3 bonded structure.

Calculated bond angles provide unambiguous evidence that the local bonding is sp^3. Referring to the labels in the figure, **∠Xea, Xeb, Yfb, Yfc, Zgc, Zgd, Zga** = 111°, 107°, 107°, 110°, 107°, 109°, 108°, and **∠eaα, ebβ, fbβ, fcγ, gcγ, gdδ, gaα** = 106°, 108°, 108°, 105°, 106°, 111°, 106°. All these are close to

the ideal tetrahedral bond angle of 109.5°.

Calculated C-Ir distances, **eX, fY** and **gZ** = 2.14 Å, 2.16 Å and 2.10Å, confirm the nature of the local graphene bonds to the surface. Indicative of chemisorption, these essentially equal the sum of the Ir metallic radius, 1.35 Å and the C covalent radius, 0.77 Å. C atoms **h, I, j and k** bond similarly to the Ir atoms beneath them, at distances 2.19 Å, 2.22 Å, 2.22 Å, and 2.16 Å. Thus, the number of C bonds to the surface Ir atoms is almost twice the number of adatoms in the island.

The Ir-C distances, **αa, βb, γc, δd** = 2.05 Å, 2.02 Å, 2.06 Å, and 2.01 Å are further indicators of the nature of the island bonding. Manifesting a typical bond-order bond-length correlation, they are all slightly smaller than the sum of Ir metallic and C covalent radii. The angles and distances quoted here, incidentally, were essentially unaffected by whether the SBZ sample used was 1×1 or 3×3.

Note that this analysis does not qualitatively distinguish island binding in the *hcp* and *fcc* regions of the moiré. The registry of C atoms relative to the first Ir substrate layer is essentially the same in both; in consequence what distinguishes the preferred *hcp* and from the less attractive *fcc* regions[7] is unclear. Computed relative energy minima do favor the *hcp* region by a minimum of 0.44 eV, among a sample of 18 ad-tetramer sites in the *hcp* and 5 in the *fcc* regions, a result in consonance with experiment.[7] Nonetheless, the qualitative physics behind it is not

yet known.[24]

In contrast to the *hcp* vs. *fcc* preference, the buckling-rehybridization picture of strong bonding *does* explain the exclusion of islands from the *atop* regions of the moiré. Therein, because C atoms reside exclusively in *fcc* and *hcp* hollows relative to the metal (cf., Fig. 3, left panel), formation of tetrahedral bonds to the surface is geometrically inhibited. In consequence, bonds do not form between C atoms and the Ir(111) substrate (see Fig. 4, right panel), island bonding, overall, is weak – for a representative ad-tetramer, *some 3.7 eV weaker* than in the *hcp* region – and adatoms prefer bridge to atop sites (see Fig. 4, left panel), to enhance their binding to the unbuckled graphene layer. Although Fig. 4 shows a flat tetramer optimized to a relative minimum energy, a trigonal pyramid is the preferred, *atop*-region morphology (cf., Table II), as that structure has an extra Ir-Ir bond. Even so, forming a 3-dimensional island is not sufficient to make *atop* regions competitive for island binding, and islands are never observed there, in equilibrium.[7]

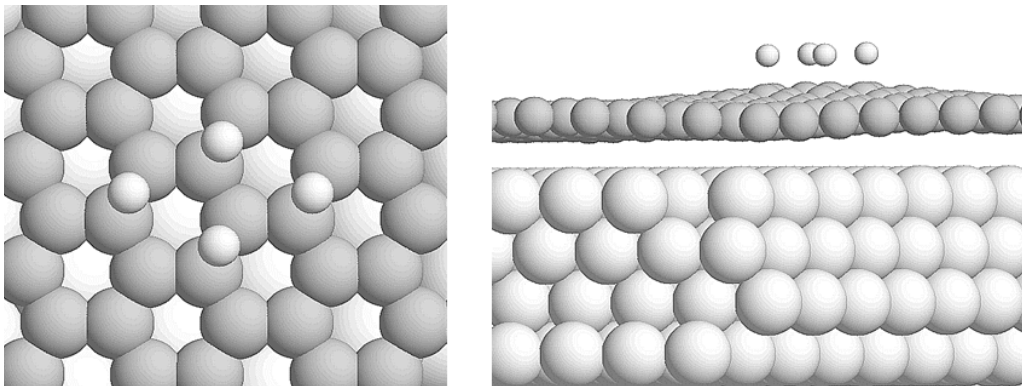

Fig. 4. Top and side views illustrating an optimized four-atom island geometry in the *atop* region of the graphene moiré. Small white balls represent Ir adatoms. Grey balls, representing C atoms, lie in 3-fold hollow sites relative to the substrate. Large white balls visible in the left-hand panel through the rings of C atoms, are the substrate Ir atoms. There is no hint of sp^3 bonding. The Ir adatoms bridge C atoms. The graphene sheet is unbuckled (contrast Fig. 4), makes no chemical contact with the substrate and, indeed, lies higher above the metal substrate where the island resides.

V) The value of mapping island site-preference energetics extensively – LDA binding energy differences are large enough, some tenths of an eV, to explain the observed stability of island arrays to 500K.[7] The scale of these differences is not a surprise. They are comparable to Ir-C bond strengths, as measured by dividing the number of Ir-C bonds (~13, in Fig. 3) into the several eV binding energy differences found between clusters in the *atop* region of the moiré, where buckling of the graphene does not occur, and in the *hcp* and *fcc* regions where it does.

Fig. 5 shows an example representative of the preference for a site in the *hcp* region. The binding of the relaxed, 19 atom hexagonal island (computed using the

3×3 SBZ sample) is 0.28 eV stronger in the *hcp* than in the *fcc* region of the moiré, while the buckling of the graphene layer, as evidenced by low lying (brown) C atoms, is confined to the immediate island vicinity, where C atoms lie directly above substrate Ir atoms. Thus, there is little doubt that sp^2 to sp^3 rehybridization accounts for the basic features of strong Ir island binding.

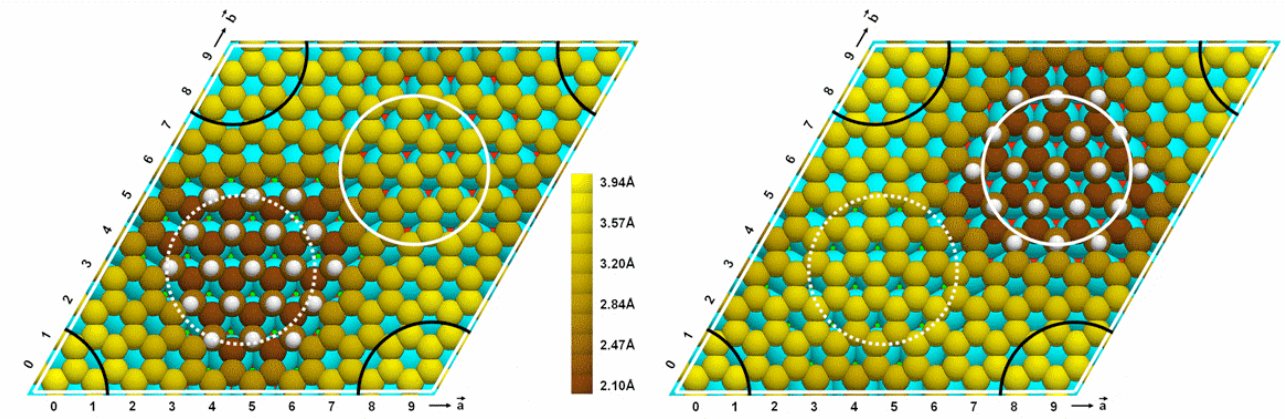

Fig. 5. (Color) Top views of 19 Ir atom islands centered in the *fcc* (left panel) and *hcp* (right panel) regions of the graphene/Ir(111) moiré. First, 2nd, and 3rd substrate layer Ir atoms are colored cyan, red and green (cf., the inset side view). This coloring shows that the solid and dotted white circles encompass the *hcp* and *fcc* regions of the moiré. Balls representing Ir adatoms are white, with radii reduced to reveal the ad-Ir registry atop C-atoms in 3-fold hollows. The color bar denotes heights measured from the average for the first Ir atom layer.

Nonetheless, centering clusters in the *hcp* or *fcc* regions of the moiré, as in Fig. 5, does not produce the highest binding energies. For example, moving the island in the right hand panel of Fig. 5 to a neighboring site less well centered in the *hcp* region, as in Fig. 6, almost doubles its LDA binding, to 0.49 eV. This

discovery warrants surveying island site energies extensively, as costly and time consuming as such an effort will be, to uncover quantitatively significant details. The color coding in Fig. 6 suggests what is at stake in the present example: the less *hcp*-centered island induces a more extensive depression of the graphene layer in its wake, a feature potentially visible in high-resolution STM images, where C atoms bind tightly to the substrate even without Ir adatoms chemisorbed above their C-atom neighbors.

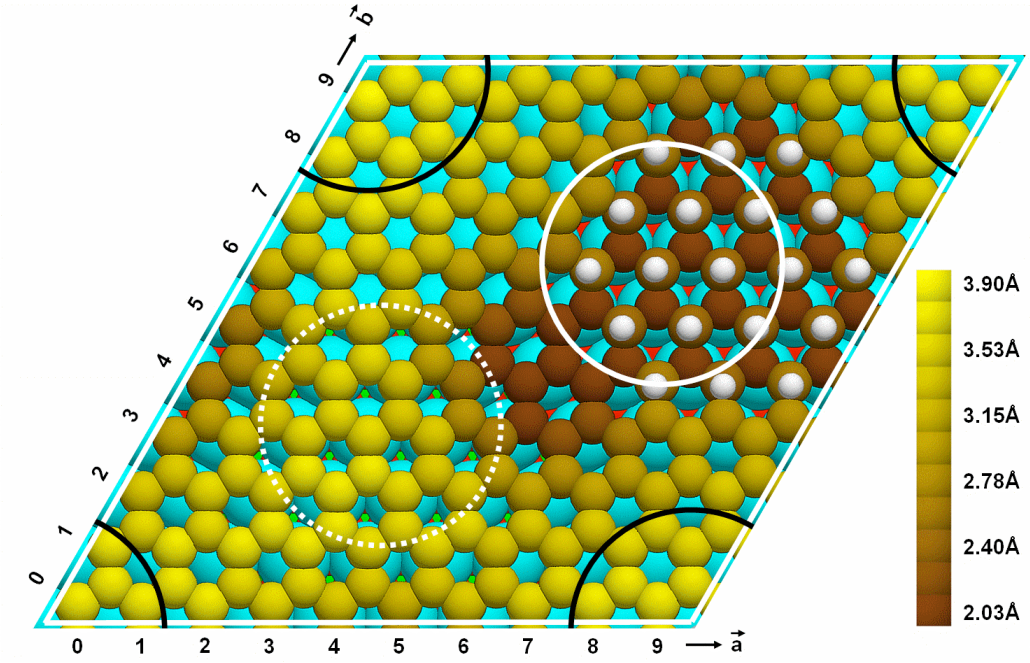

Fig. 6. (Color) Top view of a 19 Ir adatom island, a step away from being centered in the *hcp* region of the moiré. The color scheme is as in fig's 3 and 5. Note the low lying C atoms to the lower left of the island. This "trail" of improved bonding to the substrate is a clue to the characteristics of the best island binding geometries.

VI) Small islands – Ref. 7's analysis of island growth showed that whereas

ad-Ir monomers and dimers can diffuse slowly, to form larger islands, trimers and larger ad-Ir islands are immobile. These results are qualitatively consistent with sample LDA calculations reported here. To begin, Fig. 7 shows that local bonding of a trimer is very similar to that of a tetramer. The graphene layer rehybridizes to a diamond-like, sp^3 structure and chemisorbing the island to the graphene, and the graphene to the underlying Ir(111) surface.

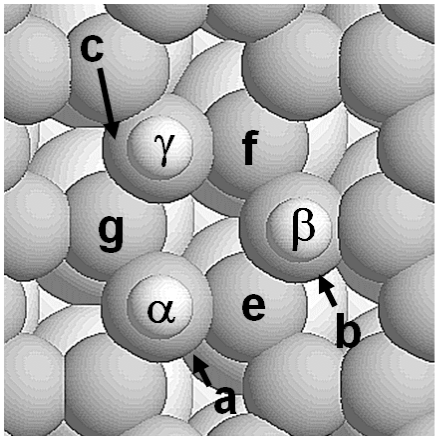

Fig. 7. An optimized Ir trimer island on the moiré. Small white balls represent Ir adatoms, grey balls represent C atoms, and large white balls are substrate Ir atoms. Compare the bonding here to that of the tetramer shown in Fig. 3.

Bonding of an Ir adatom or a dimer to the graphene layer is quite different, however, a result attributable to inadequate Ir adatom valence saturation when there are no Ir-Ir adatom bonds, or just one. An LDA optimized geometry, for an Ir monomer in the *hcp* region of the graphene moiré, is illustrated in the left panel of Fig. 8. In contrast to Ir adatoms in larger islands, the monomer sits directly above

an *atop*-site C-atom (**e** in the figure). Distances **αa**, **αb**, **αj**, and **αe** = 2.09 Å, 2.12 Å, 2.10 Å, and 2.18 Å, so that adatom **α** sits about 1.6 Å above the plane formed by **a**, **b** and **j**. Evidently, the monomer compensates for the lack of an Ir neighbor by binding to 4 C atoms of the buckled graphene layer instead of just one.

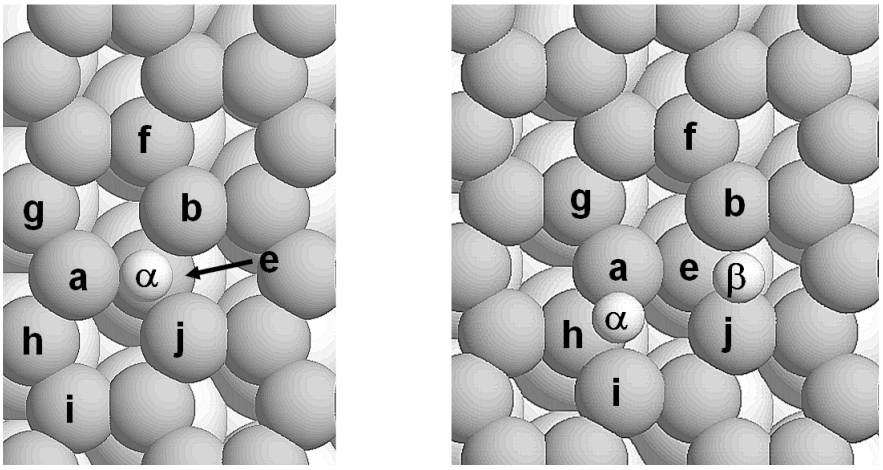

Fig. 8. Optimized geometries of an isolated Ir adatom and of an Ir ad-dimer in the *hcp* region of the moiré. Small white balls represent adatoms, grey balls represent C atoms, and large white balls are substrate Ir atoms. Compare the bonding here to that of the tetramer shown in Fig. 3, and the trimer, in Fig. 7.

In the case of an adsorbed dimer, the existence of an Ir-Ir inter-adatom bond reduces the need for bonding with p_x and p_y orbitals of the graphene layer. Accordingly, as shown in the right panel of Fig. 8, the Ir adatoms of an optimized dimer sit quasi-twofold coordinated. In the figure, distances **aα**, **hα**, **iα**, **bβ**, **eβ**, and **jβ** = 2.07 Å, 2.30 Å, 2.14 Å, 2.10 Å, 2.42 Å, and 2.07 Å.

These differences in how monomers and dimers bind to the graphene/Ir(111) substrate, as contrasted with trimers and larger ad-Ir islands, may account for simulations showing that slow diffusion of Ir monomers and dimers, fully accounts for the growth kinetics of larger ad-clusters.[7] Calculations of monomer and diffusion barriers will be the subject of future work.

VII) Discussion, tasks – The LDA results reported herein account for the Ir quantum dots observed in the *hcp* regions of the graphene/Ir(111) moiré. This qualitative success allows the inference from the computed atomic arrangements that sp^2 to sp^3 rehybridization of the graphene layer under the islands is responsible both for island adsorption and pinning of the moiré to the substrate.

This scenario is of particular interest in suggesting technological applications: Pinning means island arrays much more stable than what one might have imagined given the weak attraction of graphene layers for each other. Graphene on Ir(111) (and likely on other hexagonal transition metal surfaces) might thus serve as a template for the growth of catalytic or magnetic island arrays.

As discussed in Sec. III, Ir-C interactions in the LDA are sufficiently strong, compared to Ir-Ir bonds, that LDA calculations correctly predict that small Ir islands on the graphene/Ir(111) moiré will be flat. Not yet known is whether the LDA also accounts for the observed *upper* limit on the size of two dimensional

islands. With increasing Ir adatom coverage, the number, n, of Ir adatoms per island increases, and 3-dimensional ad-clusters begin to be observed; when $n \approx 25$, as many 2-layer as 1-layer clusters are seen.[7] Accordingly, the data suggest an energetic crossover from 2- to 3-dimensional cluster morphology at this value of n.[15] Future studies are needed to learn whether the LDA captures the crossover, as it should.

Beyond a more complete description of the static geometry of the Ir clusters on graphene/Ir(111), calculations of barriers to Ir atom, dimer and larger ad-cluster diffusion will be valuable for an analysis of the kinetics underlying the formation of Ref. 7's island structures. Possibly, that would reveal whether the differences discussed in the previous section, between monomer and dimer bonding to the graphene layer as compared to trimers and larger clusters, underlie the observation that only the former are mobile on the graphene moiré at 350K.[7]

Acknowledgment – I am pleased to acknowledge helpful correspondence with T. Michely and A. T. N'Diaye, and discussions with my colleagues, N. C. Bartelt and G. L. Kellogg. This work was supported by the DOE Office of Basic Energy Sciences, Division of Materials Science and Engineering. Sandia is operated by the Lockheed Martin Co. for the U.S. Department of Energy's National Nuclear Security Administration under contract DE-AC04-94AL85000.

VASP was developed at T. U. Wien's Institut für Theoretische Physik.

---

[1] R. Plass, J. A. Last, N. C. Bartelt, G. L. Kellogg, Nature **412**, 875(2001).

[2] R. van Gastel, N. C. Bartelt, G. L Kellogg, Phys. Rev. Lett. **96**, 036106(2006).

[3] S. Degen, C. Becker, K. Wandelt, Farad. Disc. **125**, 343(2004).

[4] M. Schmid, G. Kresse, A. Buchsbaum, E. Napetschnig, S. Gritschneder, M. Reichling, and P. Varga, Phys. Rev. Lett. **99**, 196104 (2007).

[5] N. Weiss, et al., Phys. Rev. Lett. **95**, 157204(2005).

[6] D. D. Chambliss, R. J. Wilson, S. J. Chiang, Phys. Rev. Lett. **66**, 1721(1991).

[7] A. T. N'Diaye, S. Bleikamp, P. J. Feibelman, T. Michely, Phys. Rev. Lett. **97**, 215501(2006).

[8] A. T. N'Diaye, J. Coraux, T. N. Plasa, C. Busse and T. Michely, Structure of epitaxial graphene on Ir(111), unpublished.

[9] A. T. N'Diaye, Diplomarbeit, (Rheinisch-Westfälischen Technischen Hochschule, Aachen, January 2006), unpublished.

[10] W. Kohn, L. J. Sham, Phys. Rev. **140**, A1133 (1965).

[11] P. Hohenberg and W. Kohn, Phys. Rev. **136,** B864 (1964).

[12] J.P. Perdew, in *Electronic Structure of Solids '91*, ed. by P. Ziesche and H. Eschrig (Akademie Verlag, Berlin, 1991); J. P. Perdew, J. A. Chevary, S. H. Vosko, K. A. Jackson, M. R. Pederson, D. J. Singh, and C. Fiolhais, Phys. Rev. **B46**, 6671 (1992); **B48**, 4978(1993).

[13] The LDA generally gives a better account of the lattice parameters of 5d metals than the GGA, and it also gives a far better account of the Ir(111) surface energy, and of the structure of weakly bound systems, such as graphite, according to F. Tran, R. Laskowski, P. Blaha, and K. Schwarz, Phys. Rev. **75**, 115131 (2007). For the case of graphene on the 3-d metal surface, Ni(111), G. Bertoni, L. Calmels, A. Altibelli, and V. Serin, Phys. Rev. B**71**, 075402 (2005), report reasonably good agreement with experiment in a GGA study of the spectroscopy and structure.

[14] B. S. Swartzentruber, A. P. Smith, H. Jónsson, Phys. Rev. Lett. **77**, 2518(1996).

[15] As the area of an island increases, Ir atoms on its periphery are forced to lie in regions of the moiré where alternate C atoms are no longer so close to being atop surface-layer Ir atoms. Ir-C bonding therefore benefits less from sp^2 to sp^3 rehybridization, in bigger islands, promoting the crossover to 3-dimensionality.

[16] G. Kresse and J. Hafner, Phys. Rev. **B 47**, 558 (1993); Phys. Rev. **B 49**, 14251 (1994).

[17] G. Kresse and J. Furthmüller, Comput. Mat. Sci. **6**, 15 (1996); Phys. Rev. **B 54**, 11169 (1996).

[18] P.E. Blöchl, Phys. Rev. **B 50**, 17953 (1994).

[19] G. Kresse and D. Joubert, Phys. Rev. **B 59**, 1758 (1999).

[20] D. M. Ceperley and B. J. Alder, Phys. Rev. Lett. **45**, 566 (1980), as parameterized by J. P. Perdew and A. Zunger, Phys. Rev. B **23**, 5048 (1981).

[21] M. Methfessel and A. T. Paxton, Phys. Rev. **B40**, 3616(1989).

[22] J. Neugebauer and M. Scheffler, Phys. Rev. B **46**, 16 067 (1992).

[23] J. Y. Howe, C. J. Rawn, L. E. Jones, H. Ow, Powd. Diff. **18**, 150 (2003).

[24] A persuasive story may be hard to develop. As a first attempt, one might try to follow the band-filling argument, set forth by B. Piveteau, D. Spanjaard and M. C. Desjonquères, Phys. Rev. **B46**, 7121(1992), as a way of explaining the unexpected preference of Ir adatoms for hcp hollow sites on otherwise clean Ir(111), discovered by S. C. Wang and G. Ehrlich, Surf. Sci. **246**, 37(1991).